Numerical Design Method for Water-Lubricated Hybrid Sliding Bearings

Liu Feng[1,#], Lin Bin[1] and Zhang Xiaofeng[1]

1 The State Education Ministry Key Laboratory of Advanced Ceramics and Machining Technology, Tianjin University, Tianjin, China
Corresponding Author/ E-mail: cheili@163.com, TEL: 0086-22-27404915, FAX: +0086-22-27469857

KEYWORDS : Water-lubricated, Hybrid sliding bearing, Porous restrictor, Numerical method

This paper presents a new water-lubricated hybrid sliding bearing for a high speed and high accuracy main shaft system, along with the numerical method used for its design. The porous material for the restrictor and the restriction parameter were chosen based on the special requirements of the water-lubricated bearing. Subsequent numerical calculations give the load capacity, stiffness, and friction power of different forms of water-lubricated bearings. The pressure distribution of the water film in a 6-cavity bearing is shown, based on the results of the numerical calculations. A comparison of oil-lubricated and water-lubricated bearings shows that the latter benefits more from improved processing precision and efficiency. An analysis of the stiffness and friction power results shows that 6-cavity bearings are the preferred type, due their greater stiffness and lower friction power. The average elevated temperature was calculated and found to be satisfactory. The relevant parameters of the porous restrictor were determined by calculating the restriction rate. All these results indicate that this design for a water-lubricated bearing meets specifications for high speed and high accuracy.

Manuscript received: October 18, 2007 / Accepted: December 13, 2007

NOMENCLATURE

Φ_v =permeability of porous material
A =flow areas
q_v = volume flow of water
p_s = pressure of water pump exit
p_t =pressure of oil(water) reservoir
η = kinematics viscosity of water
H =thickness of restrictor
ΔT = average elevated temperature
P_f = friction power
Q =flow
ρ = water density
C = specific heat of water

1. Introduction

The high speed and highly accurate main shaft system at the heart of a high speed machine tool directly influences the development and overall performance of that tool.[1] The most common forms of such shafts are the high speed motorized spindle, the high speed gas main shaft, and the high speed magnetic main shaft. However, the elimination of heat in the motorized spindle, the lower carrying power of the gas main shaft and the excessively sophisticated control system of the magnetic main shaft restrict their further development.[2-5]

Because of the combination of higher running accuracy, increased carrying power, and improved rigidity, the liquid-lubricated bearing is key to the development of a new type of main shaft. As a relatively new technology, the water-lubricated sliding bearing satisfies the demands of modern society for environmental conservation, health and safety, and sustainable development,[6, 7] and has therefore been quickly and widely adopted.[8, 9] Ceramic materials are used in water lubricated bearings because of their low coefficient of expansion and resistance to wear and chemical corrosion.[10] When well designed, the water lubricated bearing has the potential for high speed and accuracy.

2. Ceramic Porous Restrictor

Traditional restrictors such as the small bore, torus, and slit restrictors cannot meet the requirements of high speed and high accuracy bearings. Therefore the porous restrictor is generally used. The porous materials used in restrictors include porous metals, foam plastics, and porous ceramics. Compared with other materials, porous ceramics are ideal restrictor materials in water-lubricated ceramic bearings because of their high intensity, high rigidity, good chemical stability, and heat resistance.[11]

The characteristics of porous restrictors are as follows: high carrying capacity and rigidity, excellent stability with vibration damping under certain conditions, large flow, and hard material. The key measurement of the performance of porous restrictors, just like other types, is the restriction parameter that represents its gas permeability. The flow of pure water through porous materials can be simplified to the lamellar flow. Based on Darcy's equation, the water restriction parameter of a porous restrictor, or the volume flow of water is

$$q_v = \frac{\phi_v A(p_s - p_r)}{\eta H}. \quad (1)$$

Figure1 shows the schematic of a porous restrictor in a system.

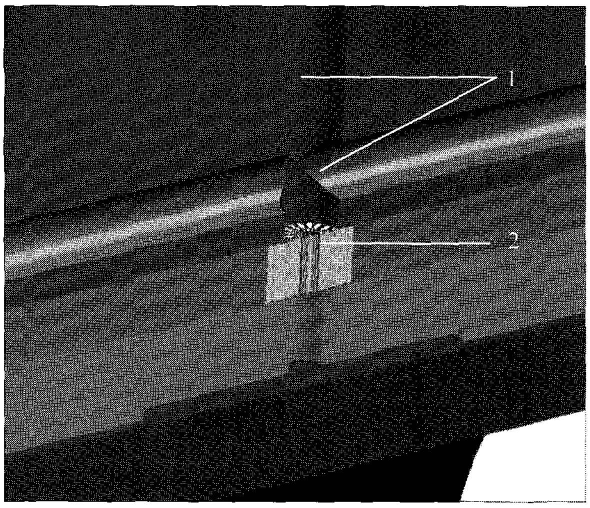

Fig. 1 Schematic of a porous restrictor in a system
(1 Water conduit; 2 Porous ceramic restrictor)

3. Numerical Computation

Combining the advantages of dynamic and hydrostatic bearings, the hybrid bearing is the first choice of water-lubricated bearing types for high-accuracy applications.[12] The methods for designing sliding bearings include analytic solutions, engineering solutions, and numerical solutions. Of these, the numerical computation using a computer program is clearly the optimal method. With a computer program that can produce solutions for every type of bearing, the optimal balance of static and dynamic bearing effects can be found to maximize the performance of the hybrid bearing.

3.1 Numerical Computation Details

The numerical computation program uses finite difference calculus to solve partial differential equations.[13] The cavity bearing is much better than the pad bearing, due to the dynamic effects that augment the carrying capacity and the rigidity. Therefore, to reduce calculation time, the program does not calculate the pad bearing parameters. It does consider 4-cavity, 6-cavity, and non-cavity bearings.

There has been considerable theoretical work on the numerical computations for hybrid slide bearings,[14, 15] and this paper does not repeat the details. Note, however, that we use the volume flow as the restriction parameter. Also note that the continuity equation needs to be reformulated, and that the pressure formula of the water film also changes during numerical computations.

Because of the boiling point of water, the temperature of the water-lubricated bearing must be calculated, and it cannot exceed 100°C. To reduce execution time, the program does not include the calculation of the whole temperature field of the bearing. The average elevated temperature is approximated from the friction power calculated by the program. Since the resistance force of the shear flow is far greater than that of pressure flow, the bearing friction power can be calculated directly from the resistance force of the shear flow.

3.2 Interpretation of Results

3.2.1 Pressure Distribution of Water Film

Figure 2 shows the non-dimensional pressure distribution of the water film in a 6-cavity bearing measured at the water pump exit p_s. This only shows axial half areas because of axial symmetry. In this figure, the bearing clearance is minimum where the pressure of the water film is the greatest. Because the depth of the water reservoir is far larger than the bearing clearance, the pressure values in the whole water reservoir are almost uniform. This means that the pressure curve of every reservoir is relatively flat.

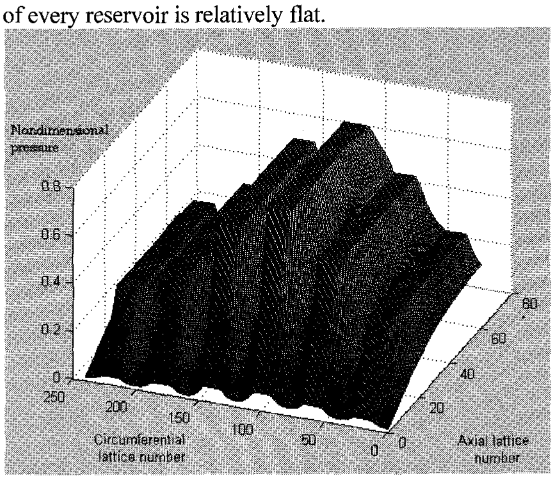

Fig. 2 Non-dimensional pressure distribution of water film for the 6-cavity bearing

3.2.2 Contrast between Oil-Lubricated and Water-Lubricated Bearings

Lubricating oil was tested to find that its density was 830 kg/m^3 and its kinematic viscosity was 10^{-5} m^2/s. The performance of a 6-cavity oil-lubricated bearing was compared to that of a 6-cavity water-lubricated bearing under the same operating conditions. The tests showed that the rigidity of the oil-lubricated form was greater than that of the water-lubricated form because the viscosity of water is lower. However, the water-lubricated bearing can still meet the rigidity requirements when its structure is optimized. For an initial bearing clearance of 20 μm, the rigidity of the 6-cavity bearing was 600 N/μm.

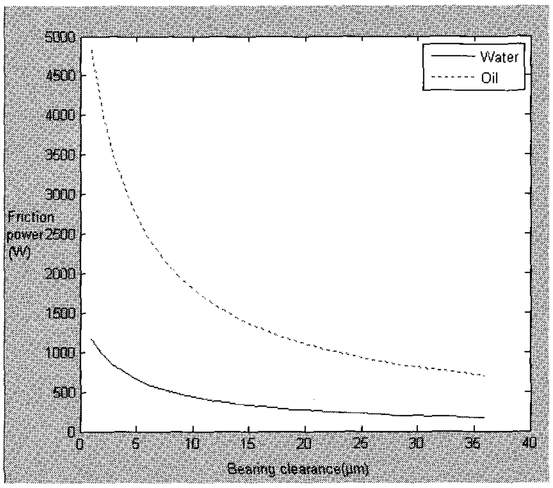

Fig. 3 Friction power versus bearing clearance

Figure 3 shows that the friction power of the oil-lubricated bearing is higher than that of the water-lubricated bearing. The high temperature caused by friction will cause the main shaft to produce serious heat denaturation, which directly and negatively affects the running and machining accuracy. A higher lubricant temperature means a lower viscidity, which also reduces the rigidity. Therefore the water-lubricated form benefits even more from improved processing precision and efficiency.

3.2.3 Rigidity

When the test was performed at a standard atmosphere pressure and at a room-temperature of 20°C, the density of water was 900 kg/m^3 and its kinematics viscosity was 2.22×10^{-5} m^2/s. Water was used as the lubricating liquid in the test. For a main shaft rotational speed of 8000 rpm, an inner bearing diameter of 80 mm, and an initial bearing clearance in the range 10–60 μm, the rigidities of 4-cavity, 6-cavity, and non-cavity bearings were calculated, and their rigidity variation tendencies were found to be the same. This shows that a smaller clearance means a higher rigidity. While the initial clearances of bearings were greater than 20 μm, the variation in their rigidities was small.

3.2.4 The Friction Power

In parallel to the conclusion in section 3.2.3, for initial bearing clearances in the range 5–60 μm, the friction power variation tendencies of the 4-cavity, 6-cavity, and non-cavity bearings were the same. The friction power of the 6-cavity bearing was the lowest of all for a given clearance. Although the rigidity of a non-cavity bearing was higher, its friction power was too high to meet precision requirements. Moreover the difference in friction powers of the different bearings was small when the initial bearing clearance is approximately 20 μm. These results mean that the preferred form is the 6-cavity bearing because it has the lowest friction power. In addition, to avoid high friction power, the bearing clearance should not be too small. On the other hand, a large clearance will reduce the rigidity. Therefore, the ideal bearing clearance should be in the range 15–25 μm.

3.2.5 Structural Optimization of the 6-Cavity Bearing

The reservoir depth: Except for the reservoir depth, the other physical dimensions of the unoptimized 6-cavity bearing and computational conditions were normal, and the working conditions were the same as in section 3.2.3. Under these conditions the rigidities and friction powers for different reservoir depths were calculated. The results show that rigidity does not vary much, but the friction power drops as the reservoir deepens. When the reservoir depth is greater than 1 mm, the variations among friction powers become small. When factors such as the ceramics processing and the flow type of liquid are considered, it is clear that the reservoir depth should be 1 mm.

The physical dimensions of the water reservoir: The inner diameter of the bearing is 80 mm, and radial rigidity of the bearing must be greater than 600 N/μm. If is unfurled on its circumference, the bearing can be divided into six chromatographic areas, where the circumferential length of every area is 41.89 mm. The width of the bearing is 40 mm.

The changes in the physical dimensions of the reservoir cause differences in rigidity and friction power because of the combined changes in static and dynamic effects. The optimal physical reservoir dimensions can be calculated to achieve the best combination of static and dynamic effects. With the optimized physical dimensions, the rigidity is 612 N/μm and the friction power is 311 W.

3.2.6 Average Elevated Temperature

The water film calorific value per unit time can be obtained once the bearing friction power has been calculated. To simplify calculations, the water flow is assumed to be adiabatic, and thus all the heat is absorbed by water from the two bearing terminal faces and the heat is balanced between the calorific value and radiating value. The average elevated temperature is given by

$$\Delta T = \frac{P_f}{Q\rho C} \tag{2}$$

Because the specific heat of water C is relatively high, the average elevated temperature given by Eq. (2) is low, $\Delta T = 7.58 \times 10^{-1}$ °C. ΔT is the unit time elevated temperature, and the whole elevated temperature in working-hours will be calculated from the data of the water circulatory system. According to exit conditions, the calculated average elevated temperature was satisfactory.

3.2.7 Relevant Parameters of the Porous Restrictor

The relevant parameters of the porous restrictor were confirmed in the program by calculating the restriction rate. The rate of permeation of the ceramic porous restrictor was 10^{-12} m^2. The external structure of the restrictor is relatively flexible, and is based on the processing factor. The specific parameters were a thickness of 5 mm and a flow area of 50 mm^2.

4. Conclusion

The development of high speed and high accuracy technology requires a new type of main shaft to reduce costs and overcome the limitations of existing types of main shaft. A new type of high speed and highly accurate main shaft supported by water lubricated technology has been presented. The form and structure of the bearing and the porous restrictor were calculated using numerical computation. The analysis of the results indicates that the design of the water-lubricated bearing meets the high speed and high accuracy specifications very well.

REFERENCES

1. Kim, S. K., "Dynamic analysis on belt-driven spindle system of machine tools," International Journal of the Korean Society of Precision Engineering, Vol. 3, No. 3, pp. 82–89, 2002.

2. Wang, C. C., Jang, M. J. and Yeh, Y. L., "Bifurcation and nonlinear dynamic analysis of a flexible rotor supported by relative short gas journal bearings," Chaos, Solitons & Fractals, Vol. 32, Issue 2, pp. 566-582, 2007.

3. Chernopyatov, Y. A., Lee, C. M., Chung, W. J. and Dolotov, K. S., "A study on the influence of nonlinearity coefficients in air-bearing spindle parametric vibration," International Journal of Precision Engineering and Manufacturing, Vol. 6, No. 1, pp.51-58, 2005.

4. Lee, S. H., Baek, Y. S. and Jung, K. S., "Modeling and analyzing electromagnets for magnetic suspension systems," International Journal of Precision Engineering and Manufacturing, Vol. 7, No. 4, pp. 28-33, 2006.

5. Ro, S. K., Kyung, J. H. and Park, J. K., "Runout control of a magnetically suspended high speed spindle using adaptive feedforward method," International Journal of Precision Engineering and Manufacturing, Vol. 6, No. 2, pp. 19-25, 2005.

6. Gerasimovl, V. S., Nikiforov, S. A. and Pautov, Y. M., "Development of high-load water-lubricated radial-axial bearings for electric-pump units in the first loop of a nuclear power plant," Atomic Energy, Vol. 89, No. 6, pp. 1027-1030, 2000.

7. Wang, G., Li, S. and Su, S., "A study on porous water hydrostatic bearings for ultraprecision applications," 21st Century Production Engineering Conference, pp. 348–352, 2001.

8. Hother-Lushington, S., "Water lubricated bearings," Tribology International, Vol. 9, Issue 6, pp. 257-260, 1976.

9. Andersson, P., "Water-lubricated and dry-running properties of ceramic journal bearings," Tribotest, Vol. 10, Issue 2, pp. 147 – 161, 2006.

10. Lu, W., Lin, B. and Cheng, X., "Study and advances in ceramic

sliding bearings with water lubrication," Bearing, No. 3, pp. 37–38, 2005.

11. Liu, P., "Introduction to cellular material," Tsinghua University Press Inc., pp. 1–24, 2004.

12. Wang, X. and Yamaguchi, A., "Characteristics of hydrostatic bearing/seal parts for water hydraulic pumps and motors, Part 1: Experiment and theory," Tribology International, Vol. 35, Issue 7, pp. 425–433, 2002.

13. Zhang, X. and Lin, B., "Theoretical research on aerostatic rectangular guideway with a finite difference method," Progress of Precision Engineering and Nano Technology, Vol. 339, pp, 371-376, 2007.

14. Park, C. H., Oh, Y. H. Lee, C. H. and Hong, J. H., "Theoretical Verification on the Motion Error Analysis Method of Hydrostatic Bearing Tables Using a Transfer Function," International Journal of the Korean Society of Precision Engineering, Vol. 4, No. 2, pp. 64–70, 2003.

15. Yoshimoto, S., Kume, T. and Shitara T., "Axial load capacity of water-lubricated hydrostatic conical bearings with spiral grooves for high speed spindles," Tribology International Vol. 31, No. 6, pp. 331–338, 1998.